

# Phase diagram of TTB ferroelectric compounds $\text{Pb}_{1-x}\text{K}_{2x}\text{Nb}_2\text{O}_6$

E.Choukri<sup>1</sup>, Y. Gagou<sup>2</sup>, D. Mezzane<sup>1</sup>, M. Elmarssi<sup>2</sup>, Z.Abkhar<sup>1</sup>, M. Elaatmani<sup>3</sup>, I. Luk'yanchuk<sup>2</sup> and P. Saint-Grégoire<sup>4</sup>

<sup>1</sup> LMCN, F.S.T.G. University Cadi Ayyad Marrakech, Morocco

<sup>2</sup> LPMC, Université de Picardie, 33, rue Saint-Leu, 80039 Amiens Cédex, France

<sup>3</sup> F.S.S. University Cadi Ayyad Marrakech, Morocco

<sup>4</sup> L2MP, UMR-CNRS 6137, Université de Toulon-Var, BP 132, 83957 La Garde Cédex, France

**Abstract:** Substitution of Pb with K in the  $\text{PbNb}_2\text{O}_6$  phases leads to a new composition of solid solution with chemical composition  $\text{Pb}_{1-x}\text{K}_{2x}\text{Nb}_2\text{O}_6$  with  $x$  ranging from 0 to 0.34 in steps of 0.05. Ferroelectric ceramics were synthesized using solid state reaction between the corresponding oxides and carbonates. Powders are pressed and heated into ceramics and their compaction is about 92%. The tetragonal tungsten bronze (TTB) structure at room temperature was confirmed by X-ray diffraction (XRD). The temperature dependence of dielectric permittivity was measured from 35 to 600°C in the  $20\text{-}10^6$  Hz frequency range.

Transition temperature decreases with the lead concentration while from  $x=0$ , with  $T_c=600^\circ\text{C}$  and to  $x=0.3$  with  $T_c=388^\circ\text{C}$ . These measurements permit to present a basical phase diagram of this family compound showing the evolution of the characteristic transition temperature  $T_c$  versus temperature. The behaviour of  $T_c$  is in agreement with theoretical study of the ferroelectric phase transition in TTB using Monte Carlo (MC) simulation. The dielectric properties of these ceramics are similar to those obtained on a single crystal and illustrate the quality of preparative conditions.

**Keywords:** ferroelectric, tetragonal tungsten bronze, phase transition, dielectric permittivity.

\*Address of Author: [el.choukri@yahoo.fr](mailto:el.choukri@yahoo.fr)

## I. Introduction

During the last years considerable attention has been focused on the study of niobates of tetragonal tungsten bronze type ferroelectrics (TTB). This structure is one of the greatest and yet purely studied families of ferroelectric oxides. They are described as a framework of  $\text{MO}_6$  octahedra ( $M$  = metal of transition, in our case  $M = \text{Nb}$ ) sharing corners, which reveals three kinds of tunnels with pentagonal (p), square (c) and triangular (t) sections [1,2]. The first two sites of coordination number respectively 15 and 12 can be occupied by ions of large size while the third one, of coordination number 9, can only be occupied by small size ions [3,4]. The structural organization is shown in Fig. 1(a) and 1(b).

One of the most known of these compounds is the lead potassium niobate with general formula  $\text{Pb}_{1-x}\text{K}_{2x}\text{Nb}_2\text{O}_6$  (PKN) and derived compounds. The reason for having interest in them is provided by their potential applications as substrate material for Surface Acoustic Wave (SAW) devices [5,6], by their non-linear optical properties and piezoelectric devices [7–10]. PKN has a large electromechanical coupling factor of bulk waves, SAW's and a small temperature coefficient of small fundamental frequencies, which was first discovered by Yamada and co-workers [11–13]. Single crystal growth, structure and dielectric properties of

$\text{Pb}_{1-x}\text{K}_{2x}\text{Nb}_2\text{O}_6$ , where  $x = 0.20$ , has been reported by Nakano and Yamada, and Hossain [13,14].

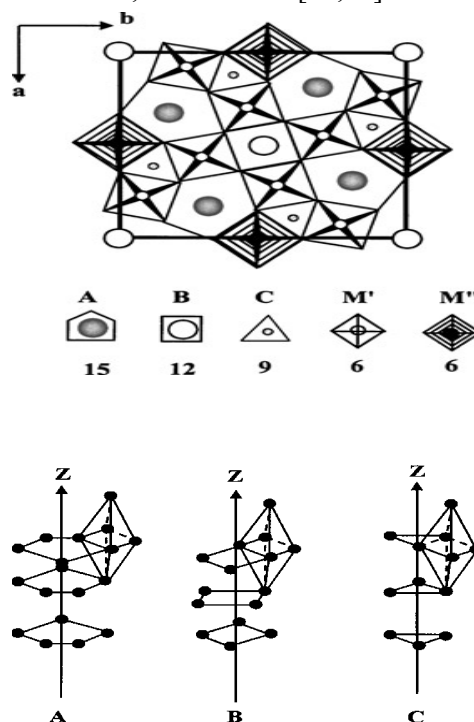


**Figure 1.** (a) Projection of the  $\text{MO}_6$  octahedra network on the plane (001) and (b) environment of the three tunnels (cavities).

For a given structural type, the value of  $T_c$  depends on the composition. The variations of  $T_c$  may be correlated with factors of chemical bonding such as size, coordination or electronic configuration of cations, bond covalency, order-disorder, etc. [15-16].

In our previous studies, compound of the family  $Pb_{2-x}K_{1+x}Li_xNb_5O_{15}$  (PKLN) of TTB-type ferroelectrics were synthesized and characterized by X-Ray and dielectric measurements. The transition temperature was shown to decrease with increasing  $x$  [17] and we have shown also that  $PbK_2LiNb_5O_{15}$  single crystal presents a dielectric anomaly at 366 °C and an unusual behaviour associated with intermediate phases. The ionic conduction related to lithium ions is evidenced in this material [18,19]. The phases  $Pb_{2(1-x)}Gd_xK_{1+x}Nb_5O_{15}$  with  $x = 0$  and  $x = 1$  were studied previously [20].

The  $Pb_{1-x}K_{2x}Nb_2O_6$  ceramic considered in the present work belongs to PKN family, which crystallizes in TTB phase. The chemical composition of PKN can also be described formally from that of  $PbNb_2O_6$  by a substitution in this compound of one of the  $Pb_{2+}$  by two ions  $K^+$ . In this paper, we focus our studies on the structure and dielectric properties changes versus the temperature for compound with general formula  $Pb_{1-x}K_{2x}Nb_2O_6$  (PKN) having a good crystallization. The relationship of the phase transition and B site substitution would be possible to elucidate as a parametric function of  $x$  in  $Pb_{1-x}K_{2x}Nb_2O_6$ . All these studies permit us to present a basal phase diagram of this family compound showing the evolution of the critical temperature versus temperature and to compare with theoretical model using Monte Carlo (MC) simulation and experimental results in  $Pb_{2-x}K_{1+x}Li_xNb_5O_{15}$  (PKLN) and  $Pb_{2(1-x)}K_{1+x}Gd_xNb_5O_{15}$  (PKGN).

## II. Sample preparation

The polycrystalline ceramic samples of  $Pb_{1-x}K_{2x}Nb_2O_6$  were prepared by solid-state synthesis. The starting materials were high-purity (99.9%) powders of oxides ( $PbO$ ,  $Nb_2O_5$ ) and carbonate ( $K_2CO_3$ ). All these materials were weighed, mixed for 1 h. The above ingredient (carbonate and oxides) were mixed in a desired stoichiometry and grounded in methanol medium for an hour with agate mortar. The powder obtained was calcined at 900°C/4h. The process has been repeated three times to achieve homogenous with single phase powder. These three heat treatments are intersected by crushing in order to obtain well homogenized mixtures. Powders of these compounds were initially compacted with a pressure of 2 ton/m<sup>2</sup> to obtain cylindrical pastille samples having 13mm of diameter and 1mm of thickness. Finally, these pastilles were sintered during 2

h between 1100°C and 1150°C. The compactness value,  $C$  (defined as the ratio between the experimental density  $d_{exp}$ , and theoretical density  $d_{theor}$ ) obtained for sintered specimens were in the range 90–92%. The diameter shrinkages of ceramics disks  $\Delta\Phi/\Phi$  were systematically determined as  $(\Phi_{init} - \Phi_{final})/\Phi_{init}$  ( $\Phi_{init}$  and  $\Phi_{final}$  represent initial and final diameter, respectively). Their values are between 0.12 and 0.15. It reveals that the PKN has a good density. All the ceramics are elaborated in the same conditions.

## III. Results and discussions X-ray studies

X-ray measurements were performed using a Bruker AXS - D8 Advanced diffractometer with a Cobalt radiations  $\lambda K\alpha_1 = 1.788970 \text{ \AA}$  and  $\lambda K\alpha_2 = 1.792850 \text{ \AA}$ . Working in transmission (Debye-Scherrer) mode, this diffractometer is provided with a cylindrical furnace which permits us to collect X-ray diagrams versus temperatures. The sample powders were sealed in a glass capillary and the transmitted beam is focused to a punctual scintillation (NaI) detector.

The crystallographic structure of the compounds was refined using the Rietveld method available in the program Fullprof [21]. Assumptions were made in the pattern matching mode, taking into account cell parameters, space groups... and instrument parameters. Results are justified by the values the minimal value of statistical standard deviation and R-factor.

The X-ray diffraction (XRD) patterns at room temperature were analyzed to confirm the symmetry and to calculate the lattice parameters for  $Pb_{1-x}K_{2x}Nb_2O_6$ . Presented in Fig.2 is the room temperature X-ray diffractogram of compound  $Pb_{1-x}K_{2x}Nb_2O_6$  ( $x=0,1$ ), which shows that this ceramic is PKLN single phase, with no traces of second phases and crystallizes with the structure of TTB.

The same quality was also achieved for all the other studied compounds. All the compositions of PKN crystallize at room temperature with an orthorhombic symmetry with space group of  $Cm2m$ , showing a small distortion of the quadratic cell about 2%, that is generally induced by the ferroelectric polarization of  $Pb_{2+}$  in the  $x$  or  $y$  direction [8]. In the case of PKN ( $x=0.1$ ), the structure was refined with a space group of  $Cm2m$  and lattice parameters of  $a = 1.7779 \text{ nm}$ ,  $b = 1.8015 \text{ nm}$  and  $c = 0.39209 \text{ nm}$ . The reported values [22] were similar to our measurements at room temperature ( $a = 1.7192 \text{ nm}$ ,  $b = 1.8014 \text{ nm}$  and  $c = 0.39147 \text{ nm}$  in PKN( $x=0.23$ ) and ( $a = 1.7526 \text{ nm}$ ,  $b = 1.8441 \text{ nm}$  and  $c = 0.3898 \text{ nm}$  in PKN( $x=0.34$ ).

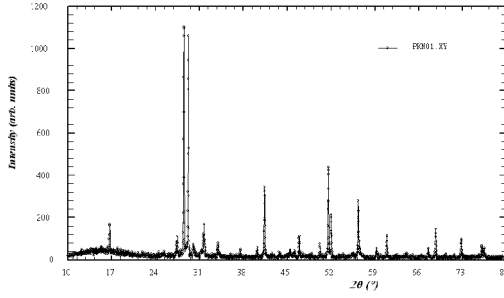


**Figure 2.** X-ray diffraction patterns of  $\text{Pb}_{1-x}\text{K}_{2x}\text{Nb}_2\text{O}_6$  composition ceramic ( $x=0.1$ ).

We report respectively in Fig. 3 the evolution of lattice parameters and unit cell volume as function of composition. The increase observed in the lattice parameters and in unit cell volume correspond to the insertion of  $\text{K}^+$  ions of big size compared to  $\text{Pb}^{2+}$  ion ( $r_{\text{K}^+} = 1.64 \text{ \AA}$ ,  $r_{\text{Pb}^{2+}} = 1.49 \text{ \AA}$ ).

#### IV. Dielectric measurements

Measurements of dielectric permittivity as a function of temperature and frequency were carried out using the LCR-meter HP 4284A, having a sensitivity of 0.05 %, which allows us to measure the capacity and the loss factor of the sample in the frequency ranging from 20Hz to 1MHz. This apparatus permits to use signal levels of ac potential and current respectively from 5mV to 2Veff and 50μA to 20mAeff. The device includes also a multimeter of HP-34401A type for measuring the temperature by means of a chromel-alumel thermocouple, which allows an accuracy of 0.2 K and a sensitivity of  $3 \times 10^{-3} \text{ K}$ . An Eurotherm-902P regulator allows us to control the speeds of sample heating and cooling during dielectric measurements. Samples are pastilles of ceramic as described previously. The lapped pellets were electroded with silver paste painted on both faces to get capacitor shaped samples.

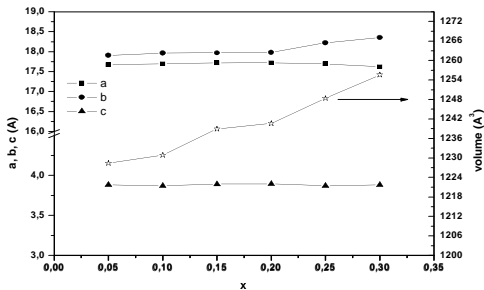


**Figure 3.** Evolution of crystalline parameters and unit cell volume versus composition.

Dielectrics measurements were performed on ceramics disks. Before measurements, silver electrodes were deposited on the circular faces of the ceramic to get

capacitor shaped samples. The dielectric constant is calculated from the following formula:

$$\epsilon = Cd/\epsilon_0 A$$

where  $C$  is the capacitance,  $d$  the thickness,  $A$  the surface area of sample and  $\epsilon_0$  is the permittivity of free space ( $8.85 \times 10^{-12} \text{ F/m}$ ).

The thermal evolution of the real part of the dielectric constant  $\epsilon'$  in the temperature range 35 - 600°C at several frequencies presents same behavior with composition (Fig. 4). The dielectric constant for all compositions ( $x=0.05$ ,  $x=0.1$ ,  $x=0.15$  and  $x=0.2$ ) above exhibits one anomaly, associated with the ferroelectric-paraelectric transition which was already observed in lead potassium niobate (PKN).

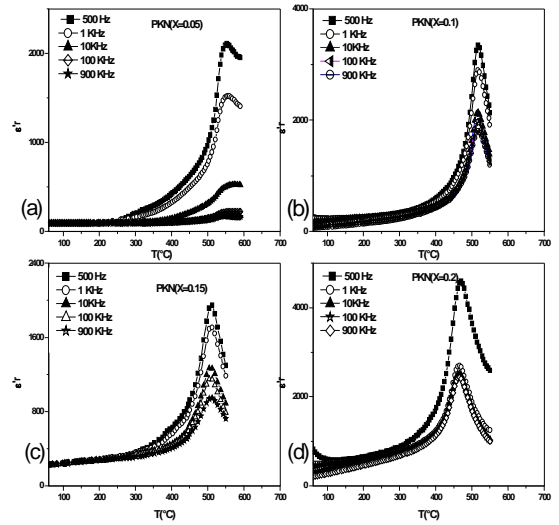


**Figure 4.** Temperature dependence of the dielectric constant in the heating mode for compounds of PKN family ( $x=0.05$  (a),  $x=0.10$  (b),  $x=0.15$  (c),  $x=0.2$  (d)) at 500 Hz, 1 KHz, 10 KHz, 100 KHz, 900 KHz.

The maximum values of  $\epsilon'$  decrease when the frequency increases. However the temperature of maximum does not depend on the frequency. This behavior is that of a classical ferroelectric, and the dispersion observed below TC cannot be due to relaxation. We attribute this dispersion to the contribution of domain walls to the permittivity of the material.

Fig. 5 shows the temperature hysteresis of the dielectric constant for different compositions observed on the left ferroelectric side of the peak in  $\text{Pb}_{1-x}\text{K}_{2x}\text{Nb}_2\text{O}_6$  after cooling-heating cycle. The same type of hysteresis of the width 8–15°C was observed for all the PKN family. We attribute this hysteresis to the first-order phase transition. Absence of discontinuity in  $\epsilon'$  and spreading of the hysteresis along all the left shoulder of the peak could signify the no uniform

distribution of transition temperatures in the ceramics. We noted that a more careful study of transition in the single-crystal of  $\text{Pb}_{1-x}\text{K}_x\text{Nb}_2\text{O}_6$  is required to confirm the nature of hysteresis and confirmed the first-order phase transition.

It is known that for a normal ferroelectric, the dielectric constant above the curie point follows the Curie-Weiss law described by :

$$\epsilon' r = C/(T-T_0) \quad (T > T_C)$$

where C the Curie-Weiss constant and  $T_0$  is the Curie-Weiss temperature.

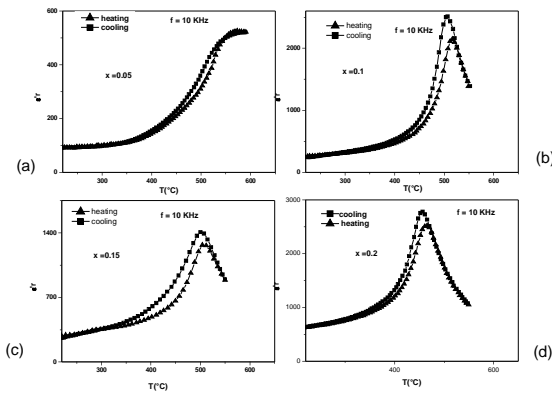


**Figure 5.** Temperature dependence of the dielectric constant  $\epsilon' r$  on cooling and on heating for  $\text{Pb}_{1-x}\text{K}_x\text{Nb}_2\text{O}_6$  ( $x=0.05$ ,  $x=0.10$ ,  $x=0.15$  and  $x=0.20$ ) at 10 KHz.

In PKN, the thermal variation of  $1/\epsilon' r$  for all compositions is of Curie-Weiss type at  $T > T_C$ . For example, Fig.6 shows the temperature dependence of  $1/\epsilon' r$  for a ceramic with composition  $x = 0.1$ ,  $0.15$  and  $0.2$  in the heating and cooling modes.

A Curie behaviour  $\epsilon' r = C/(T-T_0)$  was observed and the constant C deduced from the fit of the data on dielectric constant in the paraelectric phase, was  $C = 1.55 \times 10^5$  K. The small values of  $T_0$  ( $T_C \neq T_0$ ) for all compositions, respect to transition temperature  $T_c$  are the characteristic property of the first-order ferroelectric phase transition. The large value of C indicates that transition is mostly of displacive type.

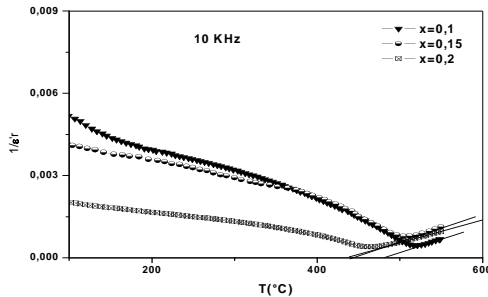


**Figure 6.** Temperature dependence of the inverse dielectric constant  $1/\epsilon' r$  for  $\text{Pb}_{1-x}\text{K}_x\text{Nb}_2\text{O}_6$  ( $x=0.10$ ,  $x=0.15$ ,  $x=0.20$ ) at 10 KHz.

The thermal evolution of the real part of the dielectric constant at 10 KHz for  $\text{Pb}_{1-x}\text{K}_x\text{Nb}_2\text{O}_6$  samples with  $0 \leq x \leq 0.3$ , presents different behaviour according to the composition (Fig.7). Several remarked variations are observed due to substitution of  $\text{Pb}^{2+}$  by  $\text{K}^+$ . Only one peak was observed in all compositions, corresponding to the phase transition of paraelectric – ferroelectric at  $T_c$ . Temperature of dielectric maximum ( $T_m$ ) decreases with x indicating  $\text{K}^+$  have entered into lattice.

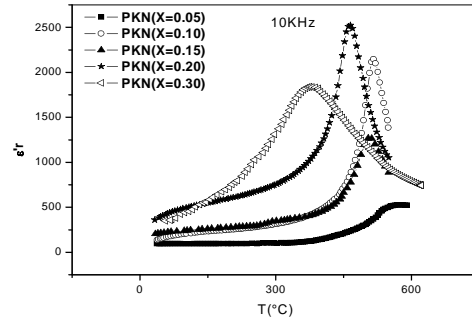


**Figure 7.** Thermal evolution of  $\epsilon' r$  for  $\text{Pb}_{1-x}\text{K}_x\text{Nb}_2\text{O}_6$  composition ceramics ( $x=0.05$ ,  $x=0.10$ ,  $x=0.15$ ,  $x=0.2$  and  $x=0.3$ )

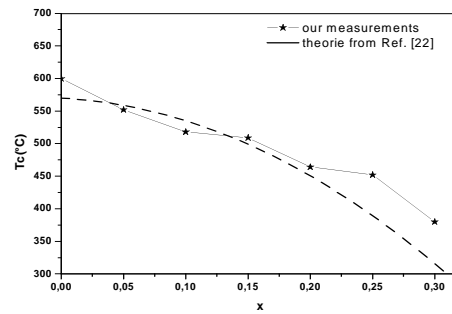


**Figure 8.** Variation of the transition temperature  $T_c$  versus composition x for the PKN family (our measurements and theory from Ref. [23]).

The Curie point of Pb-K-niobates show strong dependence on x. This dependence of x can be represented by an empirical relationship [23]:

$$T_C = 570 - (97.498)x - (2498)x^2$$

Figure 8 shows the evolution of the Curie temperature  $T_C$  (defined from  $\max \epsilon' r(T)$ ) as function of composition both for the family PKN and for the previously studied family  $\text{Pb}_{1-x}\text{K}_x\text{Nb}_2\text{O}_6$  using empirical relationship and only four values of x [23]. We observed a few decrease of  $T_C$  with K content. This behaviour is in good agreement with theoretical study of the ferroelectric phase transition in TTB using Monte Carlo (MC) simulation and also experimental results in compound of the family  $\text{Pb}_{2(1-x)}\text{K}_{1+x}\text{Gd}_x\text{Nb}_5\text{O}_{15}$  (PKGN) and  $\text{Pb}_{2-x}\text{K}_{1+x}\text{Li}_x\text{Nb}_5\text{O}_{15}$  [17]. The authors showed the similar evolution of the critical temperature versus

temperature and evidenced the existence of a morphotropic region around  $x = 0.35$  in PKGN.

## V. Conclusion

Ferroelectric compounds of TTB structure with general formula  $\text{Pb}_{1-x}\text{K}_{2x}\text{Nb}_2\text{O}_6$  ( $0 \leq x \leq 0.3$ ) (PKN) have been elaborated. All the phases are prepared by solid state reaction and are characterized by diffraction of X-rays and dielectric measurements.

Dielectric measurements show the existence of a maximum in the temperature dependence of  $\epsilon''$  for the whole family PKN that corresponds to the ferroelectric phase transition of the predominantly displacive type. According to the X-ray diffraction studies, the ferroelectric phase has an orthorhombic symmetry. Our compound exhibit many interesting features, such as shift in transition temperature and modification of dielectric proprieties with lead containing..

This work anticipates our future investigation of ferroelectric TTB family  $\text{Pb}_{1-x}\text{K}_{2x}\text{Nb}_2\text{O}_6$  that will allow us compare all obtained results on ceramics were with those on single crystal and to study the dielectric dispersion, impedance spectroscopy and electric modulus method to understand the mechanism of conduction in this ceramics.

**Acknowledgements:** This work is supported by France Foreign Ministry under N°AI/MA/07/165 and by the European project FP7=IRSES=ROBOCON.

## VI. References

Magnéli A., Arkiv Kemi, **1**, 213 (1949)  
 Y. Gagou, D. Mezzane, N. Aliouane, et al. Ferroelectrics **254**, 197 (2001)  
 Goodman G., J. Am. Ceram. Soc., **36**, 368 (1953)

Lundberg M., Sundberg M. and Magnéli A., J Solid state Chem., **44**, 32-40 (1982)  
 T.Y. Yamada, J. Appl. Phys. **46** (1975) 2894.  
 R.M. O'Connell, J. Appl. Phys. **46** (1980) 530.  
 E.A. Giess, B.A. Scott, G. Burns, D.F. O'Kane, A. Segmuller, J. Am. Ceram. Soc. **52** (1969) 276.  
 J. Ravez, B. Elouadi, Mater. Res. Bull. **19** (1975) 1249.  
 J. Thoret, J. Ravaz, Rev. Chim. Minerale **T24** (1987) 288.  
 A. Zegzouti, M. Elaatmani, Sil. Ind. **62** (7-8) (1997) 149.  
 T. Yamada, Appl. Phys. Lett. **23** (1973) 213.  
 H. Yamauchi, Appl. Phys. Lett. **32** (1978) 599.  
 J. Nakano, T. Yamada, J. Appl. Phys. **46** (1975) 2361.  
 A. Hossain, In M.S. Thesis, Texas A&M University, 1984, p. 45.  
 J. Ravez, A. Perron-Simon, P. Hagenmuller, Ann. Chim. **1**(1976) 251.  
 A. Simon, J. Ravez, C. R. Chimie **9** 1268-1276 (2006).  
 E.Choukri, Y. Gagou, E. Taifi, A. Belboukhari, M.-A. Frémy, M. Zegzouti, D. Mezzane, I. Luk'yanchuk and P. Saint-Grégoire, IMMEA-2009 Tunisie (2009).  
 Y. Gagou, D. Mezzane, N. Aliouane, T. Badèche, M. Elaatmani, M-H. Pischedda, and P. Saint-Grégoire, Ferroelectrics **254**, 197 (2001).  
 [ Y. Gagou, M.-A. Frémy, T.Badèche, D. Mezzane, E.Choukri and P. Saint-Grégoire Ferroelectrics, **371**, pp.1-4 (2008).  
 M. Oualla, A. Zegzouti, M. Elaatmani, M. Daoud, D. Mezzane, Y. Gagou, P. SaintGre'goire, Ferroelectrics **291** (2003) 133.  
 J. Rodriguez-Carvajal, Physica B **192**, 55-69 (1993)  
 W. E. Kramer and G. W. Roland, J,Crystal Growth, **58**, 393 (1982).  
 P. Jana and R. K. Pandey and D. W. Donnelly, the Eighth International Meeting on Ferroelectricity,IMF8, Gaithersburg, MD; 1993.